International Journal of Computing and Digital Systems
ISSN (2210-142X)
Int. J. Com. Dig. Sys. 9, No.1 (Jan-2020)
http://dx.doi.org/10.12785/ijcds/090111

Stability Analysis of Two Area Power System in the Presence of DDSG Wind Turbine and Fault

M. Tahir Khan Niazi[1], Arshad[1], Muhammad Ali Mughal[1]and Ashiq Hussain[1]

[1] *Department of Electrical Engineering, HITEC University Taxila, Punjab, Pakistan*

Received 09 Jul.2019, Revised 26 Dec. 2019, Accepted 30 Dec. 2019, Published 01 Jan. 2020

Abstract: The penetration of distributed generation sources in the power system has increased many folds in the last few years. This is mainly due to the technological development in solar PV and wind turbines. Although these clean renewable energy sources offer many advantages, there are certain technical challenges to operate the system in the presence of increased penetration of distributed generation. This paper investigates the effect of wind power penetration in a standard two area power system. The influence of point of interconnection of Direct Driven Synchronous Generator (DDSG) wind turbine and fault on rotor angle and synchronous frequency has been investigated. Simulation results show that the effect of fault and wind turbine on the system stability is related to the point of installment of wind turbine. It was observed that operation of DDSG wind turbine remains satisfactory under the influence of short duration fault. Furthermore, it was also noticed that point of installment of wind turbine greatly influences the synchronous frequency and rotor angle of neighboring synchronous generator.

Keywords: DDSG, wind turbine, Voltage stability, Time domain analysis, Two area power system

1. INTRODUCTION

Energy demand of the world is increasing day by day and the stress on electric power system is increasing subsequently. This calls for more energy resources, particularly clean and renewable energy resources. Using wind as a source of energy is a cherished as well as challenging task. Increasing wind power penetration will greatly affect dynamic stability of power system [1]– [5]. Therefore, it is very important to study the behavior of wind turbines under different grid conditions. When a fault occurs, then the voltage of that node decreases to almost zero depending on the severity of fault. Voltage of healthy nodes is higher and as a result, heavy current flows from healthy nodes to faulty nodes [6], [7].

Li and Chen [8] has discussed different types of wind turbine, their construction and working principle. A summary on variation in these turbines has also been discussed in the same article. Faried et al. [9] discussed different wind penetration levels and presented limits for secure wind power penetration. In [10], a mathematical model of doubly fed induction generator (DFIG) and direct driven synchronous generator (DDSG) is presented and verified by comparing response of presented model with practical scenarios. Synchronous generators are essential part of conventional power system. When a fault occurs, speed governor regulates frequency while AVR maintains the terminal voltage (reactive power) of synchronous generator. However, AVR and speed governor control is limited to the operating limits of synchronous generators [11]. Non oscillatory response of the synchronous generator can be mitigated by AVR control, and oscillations can be suppressed by using power system stabilizers(PSS)[12].Under severe fault conditions, synchronous generator controllers may not be able to cope up the situation and as a result may lose rotor angle stability or synchronization. Under such situation, it must be disconnected from rest of the power system.

Wind turbines show very poor fault ride through (FRT) capability. This is mainly due to presence of induction generator and power electronics interface inside wind turbine. FRT capability of DFIG wind turbine can be improved significantly by properly controlling the PWM convertors and by providing dynamic reactive power support [13]. The poor FRT capability of wind turbines may be due to reduced inertia of the system. Increased penetration of wind power significantly decreases the overall inertia of the power system [14]. This problem of reduced inertia of the system can be overcome by providing virtual or synthetic inertia from wind turbines. The various techniques of synthetic inertia for fully rated convertor (FRC) wind turbines are discussed in [15] for better frequency response.

Configuration of variable speed wind turbine that makes use of DDSG with permanent magnet and rotor field excitation, is quiet promising as it provides decoupled control of active and reactive power. Also, the

E-mail:mwltahirkhan@gmail.com,arshad.ali@hitecuni.edu.pk,ali.mughal@hitecuni.edu.pk,ashiq.hussain@hitecuni.edu.pk

stator frequency is independent of grid frequency. Stator convertor utilizes high frequency switching PWM convertor for attaining great degree of control with low harmonic distortion [16]. In [17], FRT capability of DDSG wind turbines is discussed. FRT capability was enhanced by providing reactive power support through grid side convertors. It was concluded that this strategy helps in maintaining transient voltage and rotor angle stability during grid fault conditions. A simplified model of converter based synchronous machine is proposed in [18] for transient and dynamic stability analysis of wind turbines.

Currently, stability assessment of wind turbines is a point of great interest for scholars and researchers around the world. A lot of work has been done regarding stability analysis of DFIG wind turbines. But less attention has been given to DDSG wind turbines. This is chiefly due to design complication of high-power convertors, being used in direct DDSG wind turbines. In this paper, time domain simulations are performed for evaluation of stability of standard two area power system in the presence of DDSG wind turbine under grid fault conditions. Time domain analysis is often used for voltage stability analysis. It provides accurate information regarding dynamics of power system. Time domain simulations are not generally used for bulky power system due to large processing time [19]. The remaining paper is organized as follows: Section II presents the time domain approach used in this work, section III and IV presents system modeling and description of the proposed setup. Section V and VI presents simulation results, discussion and conclusion.

2. TIME DOMAIN APPROACH

Dynamics of electric power system can be described in terms of swing equations. Solution of these non-linear differential equations provides information regarding stability of the system [11], [20]. Due to non-linearity of these differential equations, it is very rigorous task to find their solution. Various numerical integration methods have been developed for solving these nonlinear differential equations. Numerical integration method used here for time domain simulation is based on trapezoidal rule. Considering general differential equation as:

$$f_n\big(x(t+\Delta t), y(t+\Delta t), f(t)\big) = 0$$
$$g\big(x(t+\Delta t), y(t+\Delta t)\big) = 0$$

Here, 'f' and 'g' represent differential algebraic equation and 'f_n' is a function dependent on integration method applied. Solution of above differential equation is computed by Newton Raphson technique by iteratively calculating the increments Δx^i and Δy^i of the state and algebraic variables.

$$\begin{bmatrix}\Delta x^i \\ \Delta y^i\end{bmatrix} = -[A_c^i]^{-1}\begin{bmatrix}f_n^i \\ g^i\end{bmatrix}$$

$$\begin{bmatrix}x^{i+1} \\ y^{i+1}\end{bmatrix} = \begin{bmatrix}x^i \\ y^i\end{bmatrix} + \begin{bmatrix}\Delta x^i \\ \Delta y^i\end{bmatrix}$$

Where 'A_c^i' is a matrix depending on algebraic and state Jacobian matrix of the system. The loop terminates if the increment in the value of variable is under the defined threshold value or maximum number of iterations have reached. For trapezoidal rule,

$$A_c^i = \begin{bmatrix} I_n - 0.5\Delta t F_x^i & -0.5\Delta t F_x^i \\ G_x^i & J_{LFV}^i \end{bmatrix}$$
$$f_n^i = x^i - x(t) - 0.5\Delta t\left(f^i + f(t)\right)$$

Where 'I_n' is the identity matrix of the same dimension as of dynamic order of the system. All other matrices are Jacobian matrices of differential algebraic equations defined as;

$F_x = \nabla_x f;\ F_y = \nabla_y f;\ G_x = \nabla_x g$ and $J_{LFV} = \nabla_y g$

3. SYSTEM MODELLING

A. *Synchronous Generator*

Synchronous generator used here is rooted from Park-Concordia model and is of 6th order. A schematic diagram of it is shown in fig. 1. Network phasors and machine voltages can be represented as:

$$\mathrm{v_d} = \mathrm{V}\sin(\delta - \vartheta)$$
$$\mathrm{v_q} = \mathrm{V}\cos(\delta - \vartheta)$$

And power flow can be described as:

$$\mathrm{P} = \mathrm{v_d i_d} + \mathrm{v_q i_q}$$
$$Q = v_q i_d - v_d i_q$$

As the machine is sixth order, there are six state variables $(\dot{\delta}, \dot{e_q}, \ddot{e_q}, \dot{e_d}, \ddot{e_d}, w)$ and they can be represented in the form of equations as following:

$$\dot{\delta} = \Omega_b(w-1)$$
$$\dot{w} = \frac{P_m - P_e - D(w-1)}{M}$$

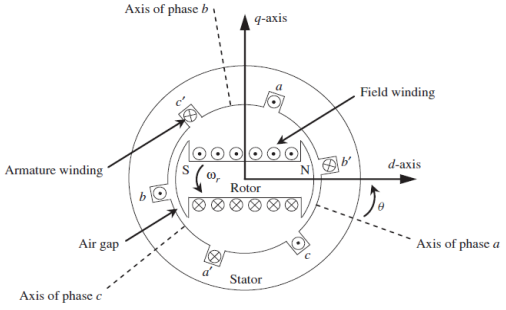

Figure 1. Synchronous machine scheme [11]

$$\dot{e_q'} = \left(-e_q' - \left(x_d - x_d' - \frac{T_{d0}''}{T_{d0}'}\frac{x_d''}{x_d'}(x_d - x_d')\right)i_d + \left(1 - \frac{T_{AA}}{T_{d0}'}\right)v_f\right)/T_{d0}'$$

$$\dot{e'_d} = \left(-f_s(e'_d) + \left(x_q - x'_q - \frac{T''_{q0}}{T'_{q0}}\frac{x''_q}{x'_q}(x_q - x'_q)\right) i_q\right) /T'_{q0}$$

$$\dot{e''_q} = \left(-e''_q + e'_q - \left(x'_d - x''_d + \frac{T''_{d0}}{T'_{d0}}\frac{x''_d}{x'_d}(x_d - x'_d)\right) i_d + \frac{T_{AA}}{T'_{d0}} v_f\right) /T''_{d0}$$

$$\dot{e''_d} = \left(-e''_d + e'_d - \left(x'_q - x''_q + \frac{T''_{q0}}{T'_{q0}}\frac{x''_q}{x'_q}(x_q - x'_q)\right) i_q\right) /T''_{q0}$$

B. Direct Driven Synchronous Generator (DDSG) Model

Schematic diagram of DDSG is shown in fig.2. It is assumedthat stator and rotor flux dynamics alter very rapidly with respect to grid dynamics and the rotational speed of generator's rotor is completely isolated from the grid. On the basis ofthese assumptions, steady state equations of DDSG can be written as:

$$v_{ds} = -r_s i_{ds} + w_m x_q i_{qs}$$
$$v_{qs} = -r_s i_{qs} - w_m (x_d i_{ds} - \Psi_p)$$

Here, 'Ψ_p' represents permanent field flux of the rotor circuit.The active and reactive power of the generator can be described as:

$$P_s = v_{ds} i_{ds} + v_{qs} i_{qs}$$
$$Q_s = v_{qs} i_{ds} - v_{ds} i_{qs}$$

Flow of active and reactive power towards grid solely depends on output current of the convertor.

$$P_c = v_{dc} i_{dc} + v_{qc} i_{qc}$$
$$Q_c = v_{qc} i_{dc} - v_{dc} i_{qc}$$

Convertor voltages are influenced by grid voltage magnitude and phase and can be expressed as

$$v_{dc} = V sin(-\vartheta)$$
$$v_{qc} = V cos(\vartheta)$$

By assuming a lossless convertor,the output power of generator becomes:

$$P_s = P_c$$
$$Q_s = 0$$

Flow of reactive power towards grid is dependent on convertor side direct current and can be related from above eq. as

$$Q_c = \frac{1}{\cos(\vartheta)} V i_{dc} + \tan(\vartheta) P_s$$

Mechanical dynamics of the DDSG can be represented mathematically as

$$w'_m = (T_m - T_e)/2H_m$$
$$T_e = \Psi_{ds} i_{qs} - \Psi_{qs} i_{ds}$$
$$T_m = \frac{P_w}{w_m}$$

Where 'P_w' is power drawn from wind and 'w_m' is rotor speed.

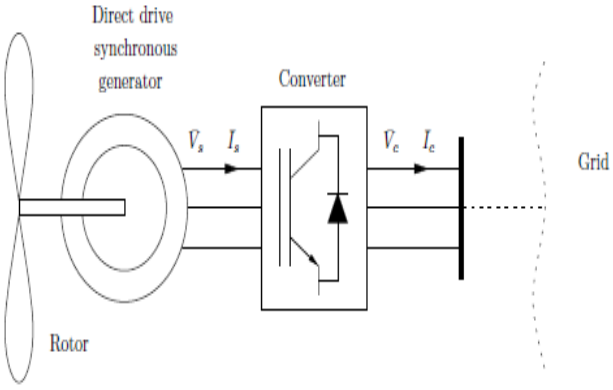

Figure 2. Schematic diagram of DDSG

Power extracted from wind (P_w) can be written as:

$$P_w = \frac{\rho}{2} C_p(\lambda, \vartheta_p) A_r v_w^3$$

Here 'ρ' is air density, 'A_r 'is area swept by rotor, 'ϑ_p' is pitch angle, 'v_w 'is wind speed, 'λ' is tip speed ratio and 'C_p' is power coefficient. Power coefficient 'C_p' can be determined from the following equation as:

$$C_p = 0.22\left(\frac{116}{\lambda_i} - 0.4\vartheta_p - 5\right) e^{\frac{-12.5}{\lambda_i}}$$

Where

$$\frac{1}{\lambda_i} = \frac{1}{\lambda + 0.08\vartheta_p} - \frac{0.035}{\vartheta_p^3 + 1}$$

4. SYSTEM DISCRIPTION

A standard two area, four machine power system [11] as shown in fig.3 was considered in this work. A MATLAB based open source toolbox, Power System Analysis Toolbox (PSAT) [21] was used for simulation. The test system consists of 4 synchronous generators, 4 transformers and 2 loads. Inertia of synchronous machine G1and G2 was set to 13s while G3 and G4 was set to 12. 35s.Six different cases were simulated, and their stability was analyzed using time domain analysis.

Case A: A standard two area, four machine system was considered, and time domain simulations were performed.

Case B: A standard two area, four machine system with a fault applied at bus 6 (area 1) and bus 10 (area 2).

Case C: The synchronous generator at bus 1 (G1) is replaced with DDSG wind turbine and a fault is applied at bus 6 (area 1).

Case D: The synchronous generator at bus 2 (G2) is replaced with a DDSG wind turbine of the same power rating and also a fault is applied at bus 6 (area 1).

Case E: The synchronous generator at bus 3 (G3) is replaced with DDSG wind turbine and a fault is applied at bus 10 (area 2).

Case F: The synchronous generator at bus 4 (G4) is replaced with DDSG wind turbine and a fault is applied at bus 10 (area 2).

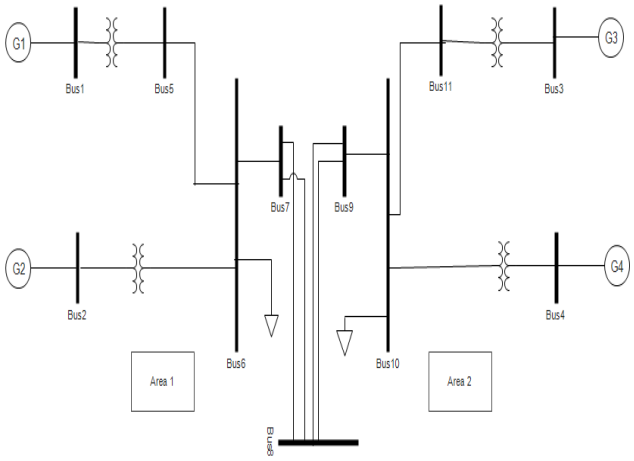

Figure 3. Two area power system

5. RESULTS AND DISCUSSION

Time domain simulations are performed for dynamic analysis of standard two area power system. Response of the power system is analyzed in the presence of DDSG wind turbine and fault. Fault is applied at 5s and cleared at 5.15s (time duration of 150ms). The steady state and dynamic stability of the system is discussed.

C. Standard two area, four machine system

In this case, standard two area four machine system is considered. Fig. 4 shows synchronous frequencies of all four generators. It can be seen that the synchronous frequencies are constant for all generators. Similarly, the rotor angles of all generators are constant as shown in fig. 5. The voltage magnitude at bus 6 and 10 are also shown in fig. 6 before any fault was applied.

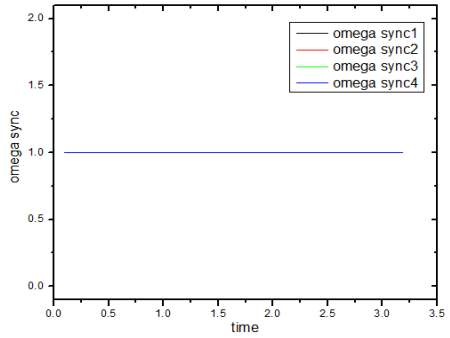

Figure 4. Synchronous frequency of all four generators

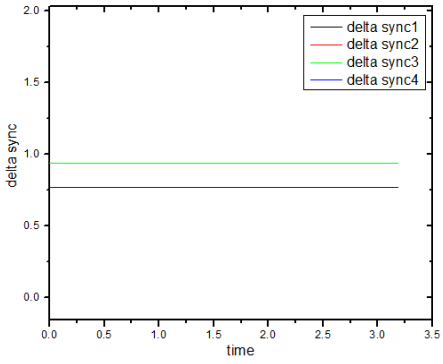

Figure 5. Comparison of rotor angle of all four generators

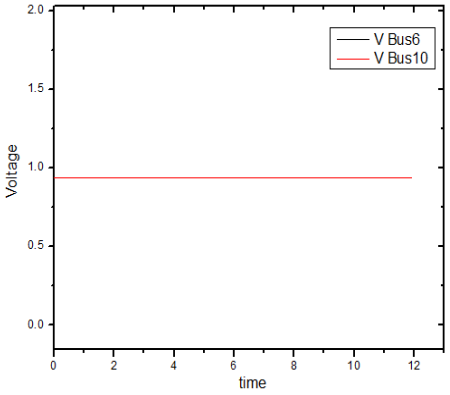

Figure.6. Voltage of bus 6 and bus 10

D. Standard two area four machine system with fault at bus 6 and bus 10

In this case, the behavior of standard two area power system is evaluated by applying fault at load buses (bus 6 & 10), separately. Firstly, a three-phase fault is applied at bus 6 for time duration of 150ms. Application of fault severely affects the rotor angle and synchronous frequency of the synchronous generators of area 1. However, system restores back to its stable condition after the removal of fault. This fact can also be verified from Fig.7, where comparison of rotor angles is made, and Fig.8, where comparison of synchronous frequency of all generators is presented.

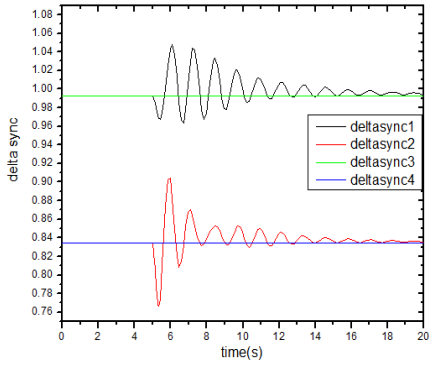

Figure7. Rotor angles of all synchronous generators (with fault applied at bus 6)

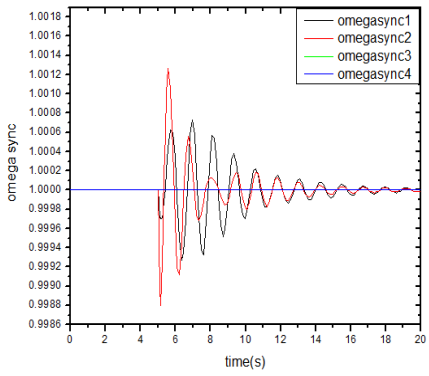

Figure 8. Synchronous frequency of all four generators (with fault applied at bus 6)

A comparison of voltage changes observed at bus 6 and 10 is given in Fig.9. It is clear from Fig.9 that application of fault at bus 6 leads to voltage sag at bus 6 and drops down to value of 0.62 p.u. Bus 10 remained stable with no changes in its voltage levels.

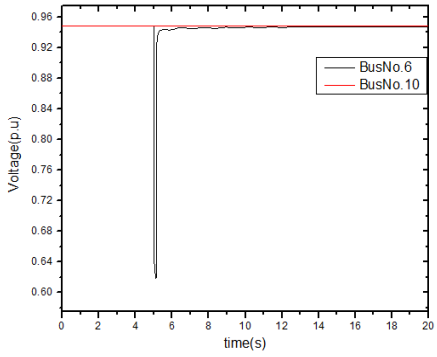

Figure 9. Voltage of bus 6 and bus 10(with fault at bus 6)

Now, fault is applied at bus 10 of standard two area power system for the same time duration. Changes observed in rotor angles and synchronous frequency of all generators is shown in Fig. 10 & 11 respectively. Similarly, variations in voltage observed at bus 6 and 10 are shown in Fig.12. It is quite evident from these results that results obtained are identical to that obtained in Fig. 7,8 and 9. Only difference is that as this time fault is applied on area 2 sides, therefore, generators on area 2 sides are affected only.

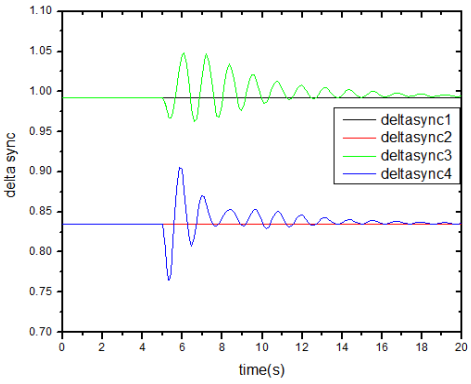

Figure10. Rotor angles of all synchronous generators (with fault applied at bus 10)

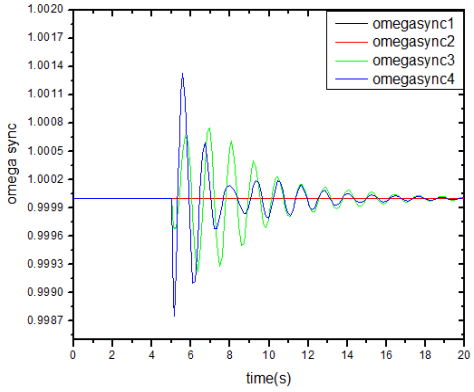

Figure 11. Synchronous frequency of all four generators (with fault applied at bus 10)

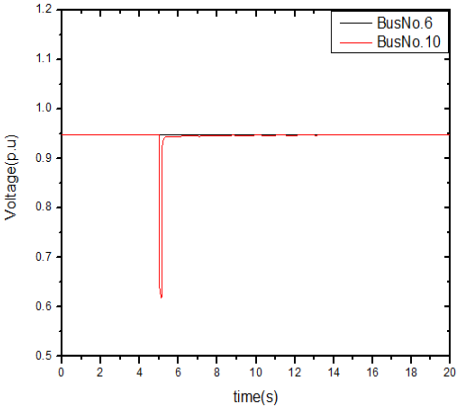

Figure 12. Voltage of bus 6 and bus 10(with fault at bus 10)

E. Generator G1 is replaced by DDSG wind turbine and a fault is applied at bus 6

In this case, performance of DDSG wind turbine is evaluated under grid dynamic conditions. Generator G1 is replaced by DDSG wind turbine of equivalent power rating. Moreover, a three-phase fault is also applied at the load bus (bus 6) of the area 1 for 150ms. Simulations are

performed to monitor dynamic changes in rotor angles and synchronous frequency of respective generators, as shown in Fig. 13 and 14 respectively.

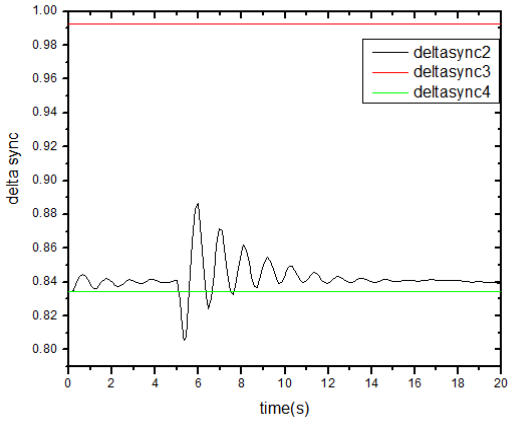

Figure13. Comparison of rotor angles

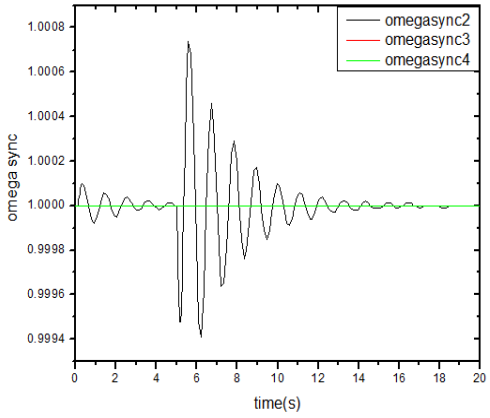

Figure 14. Comparison of synchronous frequency

A decrement in both undershoot and overshoot, in rotor angles and synchronous frequency plots (Fig.13 and 14), is observed as compare to that observed in case B. Thus, addition of DDSG wind turbine has healing effect under the influence of fault, provided it persists for short time. Synchronous frequency of generator G2 is disturbed and exhibits an overshoot of 1.00072 p.u. In the same way, after application of fault, rotor angle of generator G2 goes to its peak value of 0.884 p.u and then settles down gradually to its normal value.

Similarly, voltage sag is also observed at bus 6 as depicted in Fig.15.But, this time voltage sag observed is more dominant than that observed in case B.

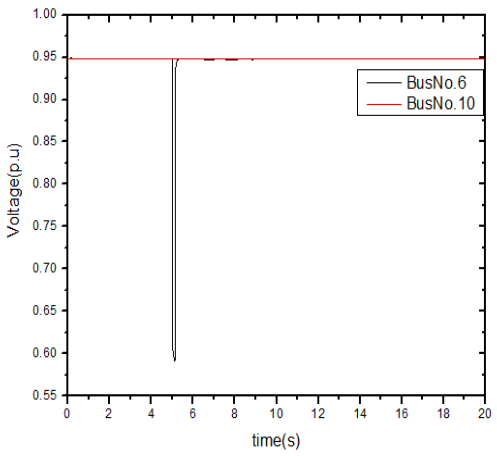

Figure 15. Voltage of bus 6 and bus 10

F. Generator G2 is replaced by DDSG wind turbine and a fault is applied at bus 6

In this case, generator 2 is replaced by DDSG wind turbine of same rating and a three-phase fault is applied at bus 6 for 150ms. Fig.16 shows that rotor angle of generator 1 decreases to 0.98 at the start and a lot of transients are observed and reaches peak value of 1.02 p.u after the initiation of fault. Fig.17 shows that the synchronous frequency of generator G1 is disturbed due to the application of fault at bus 6 and overshoot of 1.00028p.u is observed. This recorded overshoot is less than that observed in case C, where overshoot of 1.0008 is observed. However, the synchronous frequencies of area 2 generators remain unchanged. Fig.18 shows the voltage magnitudes at bus 6 and 10 and is almost identical to that observed in case C. It can be seen that steady state value of bus 6 voltage decreased to 0.57p.u from 0.94pu. Thus, during fault, a dominant decrement in voltage is observed.

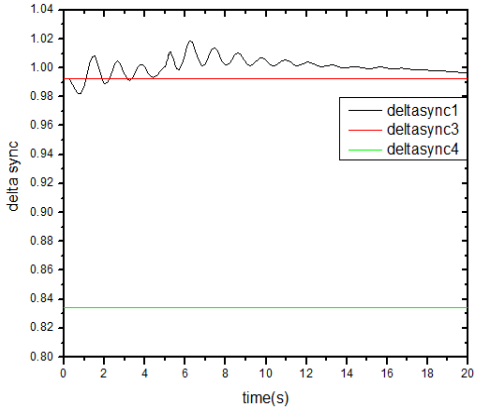

Figure 16. Rotor angles of all synchronous generators

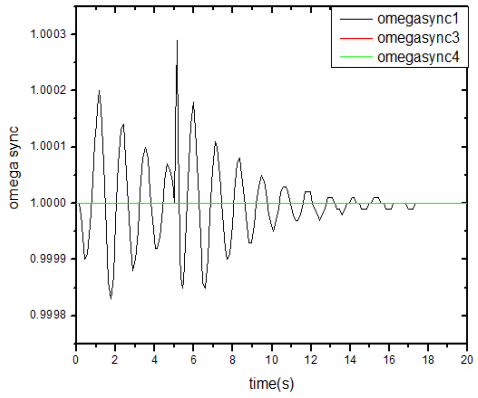

Figure 17. Synchronous frequency of generators

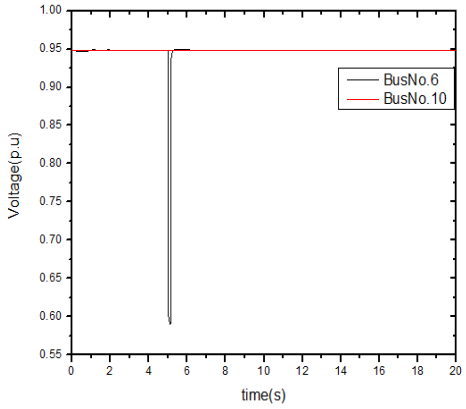

Figure 18. Voltage of bus 6 and bus 10

G. Generator G3 is replaced by DDSG wind turbine and a fault is applied at bus 10

In this case, generator G3 (of area 2) is replaced by DDSG wind turbine, under the influence of fault at bus 10. A comparison of rotor angles and synchronous frequency is presented in Fig. 19 and 20. It can be seen from these plots that addition of DDSG wind turbine under the influence of fault has severely affected the rotor angle and synchronous frequency of generator G4. Synchronous frequency of generator G4 show an overshoot of 1.0008 p.u. This overshoot recorded is identical to that observed in case C. Rotor angle of generator G4 undergoes an overshoot of 0.884p.u after introduction of fault.

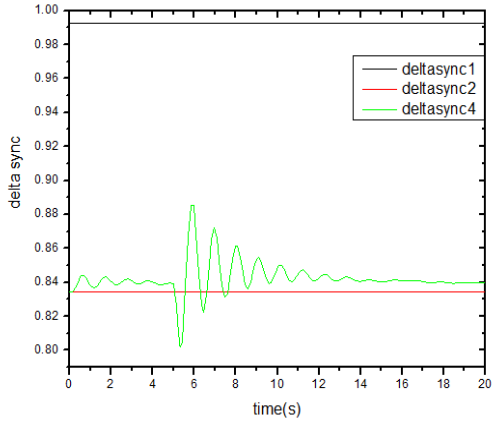

Figure 19. Rotor angles of all synchronous generators

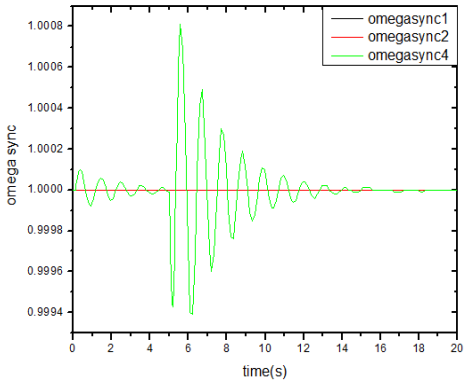

Figure 20. Synchronous frequency of generators

Voltage at bus 10 is affected because of application of fault at this bus and its voltage is dropped to 0.59 p.u. Thus, lower voltage sag is observed as compare to previous cases. Voltage level of bus 6 remains unaffected as shown below in Fig.21.

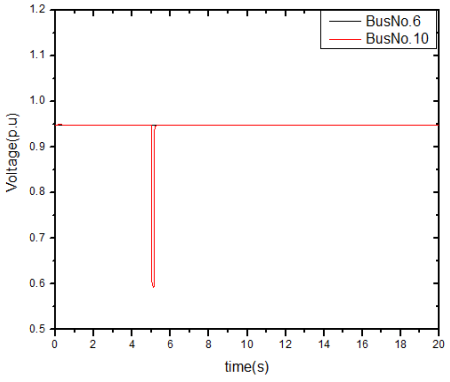

Figure 21. Voltage of bus 6 and bus 10

H. Generator G4 is replaced by DDSG wind turbine and a fault is applied at bus 10

In this case, generator 4 is replaced by DDSG wind turbine of same rating and a three-phase fault applied at

bus 10 for 150 ms. From simulation results it can be concluded that system has undergone a significant change. Rotor angle of generator 3 firstly decreases from 0.992 p.u to 0.98 p.u at the start and after application of fault shows an overshoot of 1.01 p.u and then restores down to its normal value. Similarly, its synchronous frequency shows an overshoot of 1.00022 p.u. Voltage of bus 10 has slightly decreased from 0.937p.u to 0.59 pu during fault.

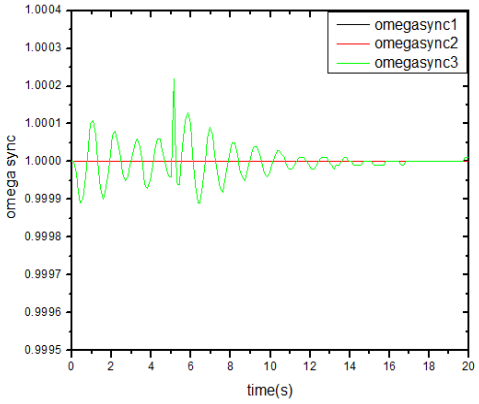

Figure 22. Rotor angles of all synchronous generators

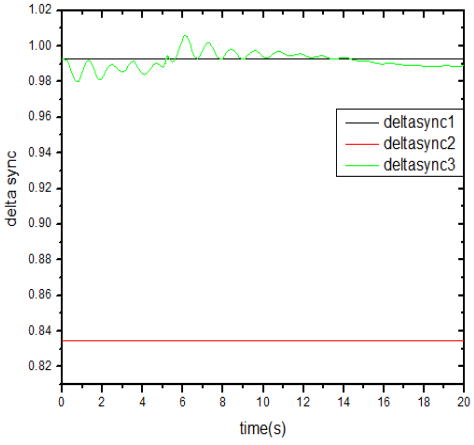

Figure 23. Synchronous frequency of generators

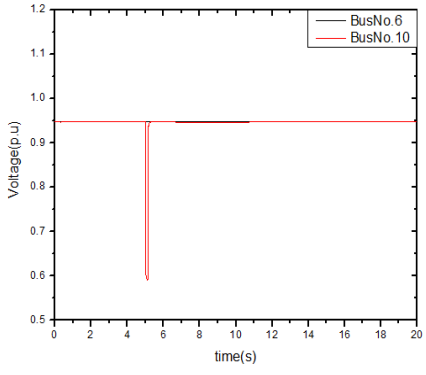

Figure 24. Voltage of bus 6 and bus 10

2. CONCLUSION

In this paper, a detailed investigation has been carried out for determining the performance of DDSG wind turbine under dynamic grid conditions. It is found that DDSG wind turbine has positive effect on stability of power system even under the influence of fault, provided it sustains for short duration. Large variations in frequency are observed in case C and E. This is because of close proximity of generator in case C and E to the fault point. While frequency deviations observed in case D and F is quite small. These results indicate that before replacing a synchronous generator with converter connected generation, feasibility study of the given system must be performed under dynamic grid conditions for ensuring better performance.

REFERENCES

[1] X. Li, J. Hui, J. Qian, P. LI, Z. XIONG, and B. XIE, "Impact of wind power generation on load modeling in distribution network," *Autom. Electr. Power Syst.*, vol. 13, p. 018, 2009.

[2] Y. Lei, W. Wang, Y. Yin, and H. DAI, "Wind power penetration limit calculation based on chance constrained programming," *Proc. CSEE*, vol. 5, no. 006, 2002.

[3] Y. Chi, Y. Liu, W. Wang, M. CHEN, and H. DAI, "Study on impact of wind power integration on power system [J]," *Power Syst. Technol.*, vol. 3, no. 31, pp. 77–81, 2007.

[4] J. Wu, S. Zhou, J. Sun, S. Chen, and Q. MENG, "Analysis on maximum power injection of wind farm connected to power system [J]," *Power Syst. Technol.*, vol. 20, no. 006, 2004.

[5] N. CAO, Y. LI, H. ZHAO, and H. DAI, "Comparison of effect of different wind turbines on power grid transient stability [J]," *Power Syst. Technol.*, vol. 9, pp. 53–57, 2007.

[6] T. K. Patel, S. K. Mohanty, and R. Chand, "A comparative study of high impedance fault in transmission line using distance relay," in *Advanced Computing and Communication Systems (ICACCS), 2017 4th International Conference on*, 2017, pp. 1–4.

[7] S. K. Mohanty and P. K. Nayak, "A comparative study of DFT and Moving Window Averaging technique of current differential protection on Transmission line," in *Advanced Computing and Communication Systems (ICACCS), 2016 3rd International Conference on*, 2016, vol. 1, pp. 1–6.

[8] H. Li and Z. Chen, "Overview of different wind generator systems and their comparisons," *IET Renew. Power Gener.*, vol. 2, no. 2, p. 123, 2008.

[9] S. O. Faried, R. Billinton, and S. Aboreshaid, "Probabilistic evaluation of transient stability of a wind farm," *IEEE Trans. Energy Convers.*, vol. 24, no. 3, pp. 733–739, 2009.

[10] J. G. Slootweg, S. W. H. De Haan, H. Polinder, and W. L. Kling, "General model for representing variable speed wind turbines in power system dynamics simulations," *IEEE Trans. Power Syst.*, vol. 18, no. 1, pp. 144–151, 2003.

[11] P. Kundur, N. J. Balu, and M. G. Lauby, *Power system stability and control*, vol. 7. McGraw-hill New York, 1994.

[12] J. L. Domínguez-García, O. Gomis-Bellmunt, F. D. Bianchi, and A. Sumper, "Power oscillation damping supported by wind power: A review," *Renew. Sustain. Energy Rev.*, vol. 16, no. 7, pp. 4994–5006, 2012.

[13] W. Qiao and R. G. Harley, "Effect of grid-connected DFIG wind turbines on power system transient stability," in *Power and Energy Society General Meeting-Conversion and Delivery of Electrical Energy in the 21st Century, 2008 IEEE*, 2008, pp. 1–7.

[14] W. Winter, K. Elkington, G. Bareux, and J. Kostevc, "Pushing the limits: Europe's new grid: Innovative tools to combat transmission bottlenecks and reduced inertia," *IEEE Power Energy Mag.*, vol. 13, no. 1, pp. 60–74, 2015.

[15] F. M. Gonzalez-Longatt, "Activation schemes of synthetic inertia controller on full converter wind turbine (type 4)," in *Power & Energy Society General Meeting, 2015 IEEE*, 2015, pp. 1–5.

[16] J. P. A. Vieira, M. V. A. Nunes, A. C. Nascimento, S. R. Silva, U. H. Bezerra, and M. M. Júnior, "Analysis of Ride-Through With the Integration of Direct Drive Synchronous Wind Generators in Power Systems," *VII INDUSCON*, 2006.

[17] A. C. Lopes, A. C. Nascimento, J. P. A. Vieira, M. V. A. Nunes, and U. H. Bezerra, "Reactive power control of direct drive synchronous wind generators to enhance the low voltage ride-through capability," in *Bulk Power System Dynamics and Control (iREP)-VIII (iREP), 2010 iREP Symposium*, 2010, pp. 1–6.

[18] S. Achilles and M. Poller, "Direct drive synchronous machine models for stability assessment of wind farms," in *4th International Workshop on Large-scale Integration of Wind Power and Transmission Networks for Offshore Wind Farms*, 2003, pp. 1–9.

[19] G. K. Morison, B. Gao, and P. Kundur, "Voltage stability analysis using static and dynamic approaches," *IEEE Trans. Power Syst.*, vol. 8, no. 3, pp. 1159–1171, 1993.

[20] P. M. Anderson and A. A. Fouad, *Power system control and stability*. John Wiley & Sons, 2008.

[21] F. Milano, "An open source power system analysis toolbox," *IEEE Trans. Power Syst.*, vol. 20, no. 3, pp. 1199–1206, 2005.

M. Tahir Khan Niazi received his B.Sc degree in Electrical Engineering from University of Engineering and Technology Lahore, Pakistan in 2017 and Master's degree from HITEC University Taxila, Pakistan in 2019. His master's research work is concentrated on wind energy integration and power quality.

Dr. Arshad received his BS degree in electronic engineering from Ghulam Ishaq Khan Institute of Engineering Sciences and Technology, Pakistan in 2011, MSc degree from University of Strathclyde Glasgow, United Kingdom in 2013 and PhD from Glasgow Caledonian University in 2017. He is currently working as Assistant Professor in HITEC University Taxila, Pakistan. Before this he worked as a Research Engineer for Whittaker Engineering Ltd. Aberdeen. His main research interests include renewable integration, high voltage engineering and electricity markets.

Dr. Muhmmad Ali Mughal has obtained his BSc degree in Electrical Engineering from Quaid-e-Awam University, Pakistan, MSc and PhD from Beihang University China in 2014 and 2018 respectively. He is currently working as an Assistant Professor in HITEC University. His current research interests include power system optimization and evolutionary algorithms.

Dr. Ashiq Hussain has obtained his BSc and MSc degreess in Electrical Engineering from UET Taxila in 1999 and 2003 respectively. He obtaiend his PhD degree from BUPT China in 2011. He is an Associate Professor and Head of Department at HITEC University Taxila. His teaching and research interest include Electrical Machines, Power Transmission and Distrubution.